

## Numerical investigation of the effect of inlet condition on self-excited oscillation of wet steam flow in a supersonic turbine cascade<sup>‡</sup>

Wu Xiaoming, Li Liang, Li Guojun<sup>\*,†</sup> and Feng Zhenping

*School of Energy and Power Engineering, Xi'an Jiaotong University, Xi'an 710049, China*

### SUMMARY

Self-excited oscillation can be induced due to the interaction between condensation process and local transonic condition in condensing flow, which is an important problem in wet steam turbine. With an Eulerian/Eulerian numerical model, the self-excited oscillation of wet steam flow is investigated in a supersonic turbine cascade. Owing to supercritical heat addition to the subsonic flow in the convergent part of the cascade, the oscillation frequency decreases with increased inlet supercooling. Mass flow rate increases in the oscillating flow due to the greater supersaturation in condensation process, while the increase will be suppressed with the flow oscillation. Higher inlet supercooling leads to the fact that the condensation process moves upstream and the loss increases. Moreover, some predictions of oscillation effects on outflow angle and aerodynamic force are also presented. Finally, heterogeneous condensations with inlet wetness and periodic inlet conditions, as a result of the interference between stator and rotor, are discussed. Copyright © 2008 John Wiley & Sons, Ltd.

Received 31 October 2007; Accepted 28 August 2008

KEY WORDS: self-excited oscillation; wet steam; turbine cascade; condensation; inlet supercooling; numerical research

### 1. INTRODUCTION

Effects of inlet condition on self-excited oscillation of wet steam flow in a supersonic turbine cascade are investigated numerically in this paper. Phase transition of steam from gas phase to liquid phase by condensation occurs in non-equilibrium state as the nucleation is homogeneous (where the condensation nuclei form in the gas phase itself) and the cooling process is fast enough.

---

\*Correspondence to: Li Guojun, School of Energy and Power Engineering, Xi'an Jiaotong University, Xi'an 710049, China.

†E-mail: liguojun@mail.xjtu.edu.cn

‡This article was published online [23 October 2008]. Some errors were subsequently identified. This notice is included in the online and print versions to indicate that both have been corrected [31 October 2008].

In non-equilibrium condensing flow the self-excited oscillation is observed, which is caused by the interaction between the condensation process and local transonic flow.

This phenomenon was first discovered by Schnerr in 1962 in slender nozzle expansion flow of moist air. Subsequently, it was reported again in pure steam flow by Barschdorff and Filippov [1] in 1970. Barschdorff obtained the frequency of homogeneously condensing flows of moist air (1967) and pure steam (1971) based on the experimental results. He found a monotonically increasing frequency dependence on the water vapor content in the supply. The first similarity law for the dimensionless frequency of self-excited oscillations was derived by Zierp and Lin for a constant nozzle throat height, different expansion rates and varying supply conditions in 1968.

In Laval nozzle, the formation mechanism of the self-excited oscillation is clear now. Generally, as reported in most experimental and numerical researches [2–4], the self-excited oscillation occurs in the divergent part of nozzle, in which the heat release during condensation process makes supersonic flow return to subsonic condition. For the supersonic flow with a definite Mach number  $Ma$ , the critical amount of heat  $Q_c$  is required to return the flow to sonic condition. For a given nozzle, the condensation process is determined by the inflow conditions leading to the fact that the amount of heat addition  $Q$  to the supersonic flow is also determined. Under subcritical heat addition ( $Q < Q_c$ ), the condensation results in a small pressure rise, the so-called ‘condensation shock’, and the flow is stable. For supercritical heat addition ( $Q \geq Q_c$ ), an aerodynamic shock is embedded in the zone of rapid condensation, and it is enhanced with the increase of  $Q$ , but the flow is still stable. Under ultra supercritical heat addition ( $Q \gg Q_c$ ), the aerodynamic shock moves upstream. As a result, the upstream temperature of the rapid condensation zone rises and the condensation intensity is weakened, which is followed by the decrease of the heat release. Therefore, the condition leading to the aerodynamic shock is broken. The supercooling in the condensing flow rises once more and the condensation swells; therefore, the above cycle repeats, which is called ‘self-excited oscillation’.

It can be seen that the self-excited oscillation is caused by the interaction between the condensation process and the local transonic flow. Such a condition exists in wet steam turbine; therefore, the self-excited oscillation is also likely to happen in steam turbine. It not only makes the flow more complicated, but also endangers the safety of structure. In fact, due to impurities in real steam turbine stage and may be droplets in upstream wakes, the non-equilibrium state of the condensation process is weakened; therefore, the possibility of self-excited oscillation is reduced. However, Dobkes *et al.* [5] conducted measurements on the stress of the rotor blade in an experimental steam turbine. They found that when the unsteady flow is observed in the turbine cascade, the stress of the rotor blade increases 1.5–2 times. It was concluded that the self-excited oscillation in the turbine cascade takes place. Whirlow *et al.* [6] observed non-synchronous rotor blade vibrations in a steam turbine, which may also be attributed to condensation-induced oscillation in partial region of the cascade passage.

For steam turbine, the self-excited oscillation not only leads to the vibration of blade, but also produces additional losses, including the aerodynamic shock loss due to supercritical heat addition and that caused by separation of boundary layer interacting with aerodynamic shock besides the well-known non-equilibrium loss.

The progress in the study of the self-excited oscillation in wet steam turbine is slow due to the complex nature of this problem. Few experimental results have been published. Most published numerical researches are limited to the unsteady flows in nozzles [2–4]. Li *et al.* [7] studied the stable limit of wet steam flow and the self-excited oscillation in a supersonic turbine cascade by

numerical approach. Moreover, the effects of flow oscillation on the aerodynamic performance of the cascade and the characteristics of the blade strength are also discussed.

For a given nozzle or turbine cascade, the condensation process is determined by the inflow conditions, which also determines the characteristics of self-excited oscillation including occurrence, position, frequency and intensity. In this paper, the self-excited oscillating flow in the above supersonic turbine cascade is studied numerically based on the research in literature [7]. Oscillation mechanism with condensation in the convergent part of the cascade is studied. Frequency, mass flow rate, outflow angle, loss and force on the blade are discussed at different inlet supercooling. The equilibrium condensation with inlet wetness and the periodic inlet conditions, as a result of stator rotor interaction, are also investigated numerically and analyzed.

## 2. MATHEMATICAL MODEL

The condensing flow of wet steam can be treated as a two-phase system as follows. The primary phase is the gaseous phase consisting of water vapor, while the secondary phase is the liquid phase consisting of condensed-water droplets.

The following assumptions are made in this model:

- (1) The velocity slip between the droplets and the gaseous phase is negligible.
- (2) The interactions between droplets are neglected.
- (3) The mass fraction of the condensed phase,  $Y$  (also known as wetness factor), is small ( $Y < 0.2$ ).
- (4) Owing to the small size of droplets (the radius is approximately  $0.02\text{--}2\mu\text{m}$ ), the volume is negligible.
- (5) The inter-phase drag force is neglected.

From the preceding assumptions, an Eulerian/Eulerian model can be established. The conservation equations of mass, momentum and energy for the gaseous phase are

$$\frac{\partial \rho_g}{\partial t} + \frac{\partial(\rho_g u_j)}{\partial x_j} = -\rho \dot{m} \quad (1)$$

$$\frac{\partial(\rho_g u_i)}{\partial t} + \frac{\partial(\rho_g u_i u_j)}{\partial x_j} = -\frac{\partial p}{\partial x_i} + \frac{\partial \tau_{ij}}{\partial x_j} - \rho \dot{m} u_i \quad (2)$$

$$\frac{\partial(\rho_g E_g)}{\partial t} + \frac{\partial(\rho_g E_g u_j)}{\partial x_j} = -\frac{\partial(p u_j)}{\partial x_j} + \frac{\partial(u_i \tau_{ij} - q_j)}{\partial x_j} - \rho \dot{m} (h_t - h_{fg}) \quad (3)$$

where the source terms  $-\rho \dot{m}$ ,  $-\rho \dot{m} u_i$  and  $-\rho \dot{m} (h_t - h_{fg})$  are introduced to count the interactions between the gaseous and liquid phases. The condensate mass rate  $\dot{m}$  is expressed as

$$\dot{m} = (1 - Y) J \rho_1 \frac{4\pi r_c^3}{3} + 4\pi r^2 \frac{dr}{dt} \rho_1 N \quad (4)$$

where the nucleation rate  $J$  and the droplet growth rate  $dr/dt$  are determined by the classical condensation theory and the same expressions as published in [2] are adopted. In addition, the virial equation for water vapor is employed to make the equation set enclosure and is expressed as

$$p = \rho_g RT(1 + B\rho_g + C\rho_g^2) \quad (5)$$

As mentioned above, the velocity slip between the two phases can be neglected; hence, only the equations describing the quantity and size of droplets are required additionally for the liquid phase. The conservation law yields

$$\frac{\partial(\rho N)}{\partial t} + \frac{\partial(\rho N u_j)}{\partial x_j} = \rho_g J \tag{6}$$

$$\frac{\partial(\rho Y)}{\partial t} + \frac{\partial(\rho Y u_j)}{\partial x_j} = \rho \dot{m} \tag{7}$$

Based on the solution of  $N$  and  $Y$ , the mean radius  $r$  can be determined by the following equation:

$$r = \sqrt[3]{3Y/(4\pi\rho_l N)} \tag{8}$$

The overall concentration of water droplets in wet steam follows the Boltzmann distribution law [8]. Therefore, describing the liquid phase in condensing flow with the state parameters  $N$  and  $r$  in statistical macro-average, which is adopted in this paper, is equivalent to the polydispersed method.

Therefore, with Equations (1)–(3) and (6)–(8) the wet steam flow with condensation can be solved. The finite volume method and the explicit time-marching technique are used. The second-order upwind scheme is adopted in the spatial discretization. Furthermore, for the time-dependent problem, the dual time stepping method is applied.

### 3. VALIDATION OF THE MODEL

First, the wet steam flow with condensation in a Laval nozzle was simulated to validate the numerical model. Predictions of nozzle centerline pressure and droplet size are compared in Figure 1 with experiment for nozzle B of Moore *et al.* [9]. It can be seen that the numerical model properly predicts the characteristics of the wet steam flow with condensation in this nozzle.

Second, the condensing flow with self-excited oscillation in a Laval nozzle was simulated. Skilling *et al.* [3] conducted experimental investigation on the condensing flow in the nozzle. The

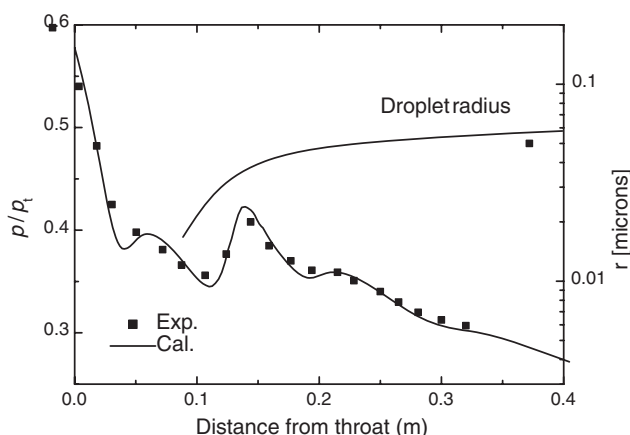


Figure 1. Comparison of centerline pressure and mean droplet size with the experiments of Moore *et al.* [9] (nozzle B). Inlet conditions  $p_{01} = 25\,000\text{ Pa}$ ,  $T_{01} = 358\text{ K}$ .

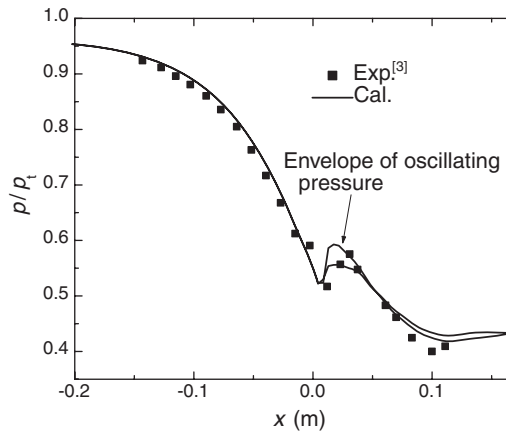


Figure 2. Comparison of centerline pressure with the experiment of Skilling *et al.* [3]. Inlet conditions  $p_{01} = 35\,140\text{ Pa}$ ,  $T_{01} = 347.9\text{ K}$ .

Table I. Characteristics of oscillating flow on the test point, which is on the wall and the location is 30 mm behind the throat.

	$f$ (Hz)	$\Delta p$ (Pa)
Exp. [3]	380.0	1976
Cal.	378.4	1947

pressure distribution along the nozzle centerline is shown in Figure 2. It can be seen that the flow is oscillating in the rapid condensation zone immediately behind the nozzle throat, which is caused by the interaction between the condensation process and the local supersonic flow as described previously.

The frequency  $f$  of the oscillating flow is given by the Fast Fourier Transform analysis and listed in Table I. The calculated frequency is 378.4 Hz, which agrees well with the experimental value 380 Hz. The amplitude  $\Delta p$  of the oscillating pressure in the rapid condensation zone is also listed in Table I. The experimental value on the test point is 1976 Pa and the numerical simulation gives 1947 Pa. It can be seen that the numerical model properly predicts the characteristics of the self-excited flow oscillation in this nozzle.

#### 4. THE SELF-EXCITED OSCILLATING FLOW IN A SUPERSONIC TURBINE CASCADE

In large-scale turbine, the flow near the blade tip in the low-pressure turbine stages is in transonic condition, which can induce the phenomenon of self-excited oscillation. Based on the numerical model presented in this paper, the oscillation flow in a supersonic turbine cascade is analyzed at different inlet supercooling. The geometry of the cascade is given in Figure 3. Three points marked as A, B and C in the divergent part of the cascade passage are set to monitor the oscillation parameters.

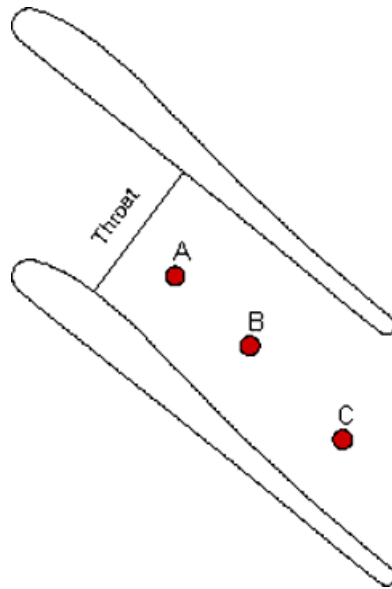


Figure 3. Geometry of the supersonic turbine cascade. The center point of the throat line is located at (0,0) and the three points are located at (10.2, -12.5), (28.3, -30.0), (54.0, -53.8), respectively. (Unit: mm).

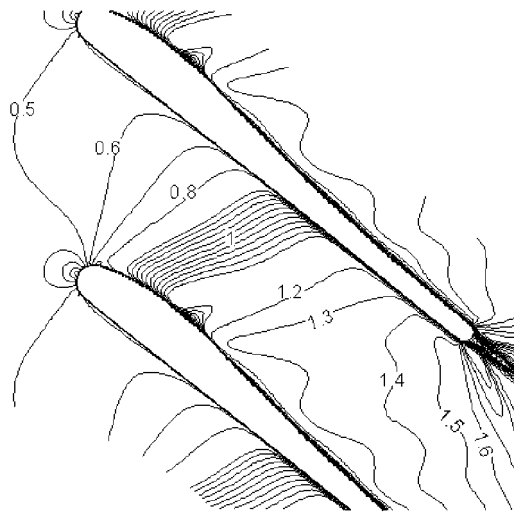


Figure 4. Isograms of the Mach number for single phase flow. Increment of the iso-lines  $\Delta Ma = 0.02$  when  $0.9 < Ma < 1.1$ ; otherwise,  $\Delta Ma = 0.1$ . Flow conditions  $p_{01} = 35\ 140\text{ Pa}$ ,  $T_{01} = 397.3\text{ K}$ ,  $p_b/p_{01} = 0.38$ .

#### 4.1. The aerodynamic characteristics of the cascade

First, the aerodynamic characteristics of the cascade are investigated. At the suction side the expansion rate near the throat of the cascade is relatively high, but it decreases to nearly zero downstream, whereas it is nearly constant at the pressure side. The isogram of the Mach number in single phase flow is shown in Figure 4. It can be seen that the cascade is fore-loaded.

#### 4.2. The oscillation mechanism in the cascade

Self-excited oscillation flow occurs in the cascade with the inlet supercooling  $\Delta T_{01} = 6.1\text{K}$ . Isograms of log nucleation rate for one period of self-excited oscillation are shown in Figure 5(a). Owing to the expansion rate, condensation occurs near the throat at the suction side, while it occurs behind the throat at the pressure side ( $t = 0$ ). Owing to supercritical heat addition at the suction side, the rapid condensation zone moves upstream, and then the upstream temperature rises, which leads to the fact that the condensation process ahead of the throat is weakened ( $t = 0.125T$ ). As a result, a secondary condensation occurs downstream at the suction side due to the high expansion rate near the throat, while a new rapid condensation zone (which can be also regarded as a secondary condensation) forms downstream at the pressure side due to the expansion rate, which is nearly constant ( $t = 0.25T$ ). With further weakening of the condensation process ahead of the throat, the two previous condensation zones move downstream and disappear finally ( $t = 0.375\text{--}0.5T$ ). Owing to the decrease of latent heat release near the throat, the upstream supercooling rises, and then the condensation process is enhanced once more ( $t = 0.5\text{--}0.875T$ ).

Corresponding isograms of the Mach number are shown in Figure 5(b). It can be seen that the critical section locates behind the throat due to the heat release in the convergent part, and its position is determined by the amount of latent heat release. The subsonic flow near the throat is heated to supersonic at the suction side; therefore, a weak shock builds up behind the rapid condensation zone ( $t = 0$ ), and it moves upstream with the increase of latent heat release ( $t = 0.125T$ ). In the convergent part of the cascade, the shock is slightly enhanced first ( $t = 0.125T$ ), but it is weakened and disappears immediately due to the weakening of the upstream condensation process ( $t = 0.25T$ ). Meanwhile, two strong shocks build up in the two secondary condensation zones. Owing to the much higher Mach number ahead of them, the shocks move downstream, in spite of the stronger condensation process and shock intensity. Therefore, they are enhanced in the divergent part first ( $t = 0.375T$ ). Especially due to the expansion rate, the shock at the pressure side disappears immediately ( $t = 0.5T$ ), while the other one is weakened gradually ( $t = 0.5\text{--}0.875T$ ). On the other hand, the critical section moves downstream and disappears in the outflow, while at the same time a new one builds up behind the throat ( $t = 0.5T$ ).

Generally, the frequency of self-excited oscillation in nozzles is determined mainly by the condensation intensity near the centerline. Even with high wall curvature, near nozzle wall the locally stronger temperature gradient tends to stabilize the flow [4], but its effect is limited in the downstream flow near the wall, barely to the main flow. However, in the present cascade the weakening of the condensation process ahead of the throat can lead to the downstream secondary condensation. Therefore, the oscillation frequency is determined mainly by the variational rate of the upstream condensation process, which is determined by the supercritical heat addition near the throat at the suction side.

The subsonic condition allows the oscillation pressure in the rapid condensation zone to spread upstream. As a result, the inlet mass flow rate varies periodically. Supposing that the cascade has unit spanwise height, the time history of mass flow rate is shown in Figure 6. Although the

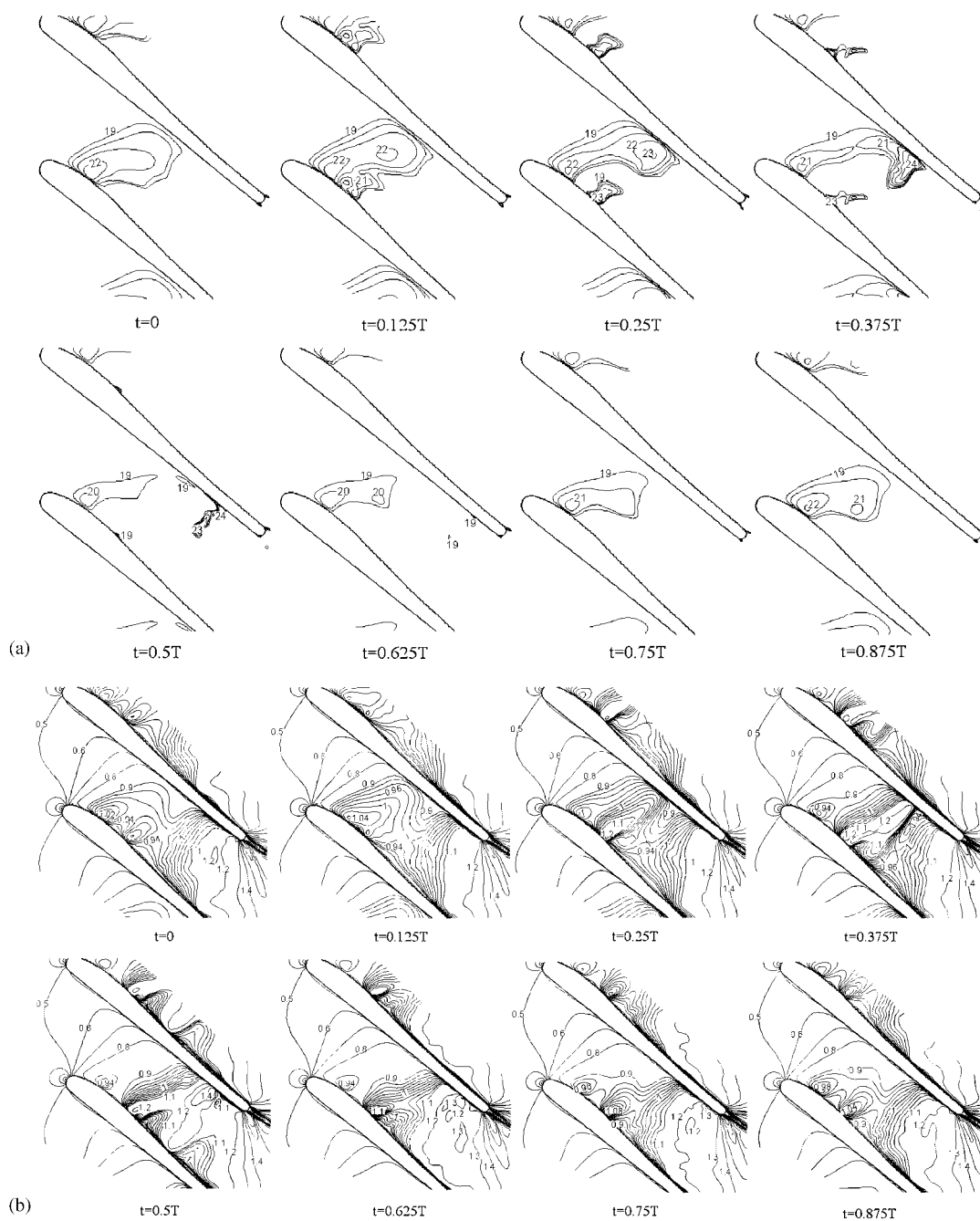


Figure 5. (a) Isograms of  $\log(J)$  for one period of self-excited oscillation. Increment of the iso-lines  $\Delta \log(J) = 1$ . Flow conditions  $p_{01} = 35\,140\text{ Pa}$ ,  $\Delta T_{01} = 6.1\text{ K}$ ,  $p_b/p_{01} = 0.38$ . ( $T$  is the time for one period oscillation) and (b) isograms of the Mach number for one period of self-excited oscillation. Increment of the iso-lines  $\Delta Ma = 0.02$  when  $0.9 < Ma < 1.1$ ; otherwise,  $\Delta Ma = 0.1$ .



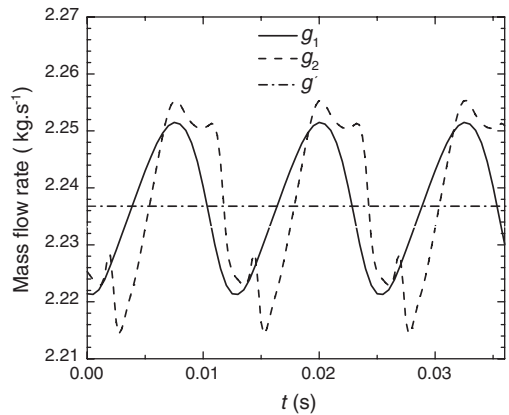


Figure 6. Time history of mass flow rate, where  $g_1$ ,  $g_2$  and  $g'$  are at inlet and outlet sections, the time-averaged value, respectively.

time-averaged mass flow rates at the inlet section and outlet section are identical, the variations of mass flow rate at these two sections are not synchronous. The difference indicates the periodical compression and expansion of wet steam in the cascade passage [7].

#### 4.3. The limit of steady flow

Calculations were implemented to investigate the inlet supercooling conditions leading to self-excited oscillation. Keeping the pressure ratio  $p_b/p_{01}=0.38$  constant, the inlet supercooling  $\Delta T_{01}$  increases from  $-0.9$  to  $11.1$  K. The oscillating flow is observed when  $0.6\text{ K} \leq \Delta T_{01} \leq 9.1\text{ K}$ ; otherwise, the flow keeps steady.

The dynamics of the self-excited flow oscillation for the supersonic cascade is given in Figure 7. The rapid condensation zone locates behind the throat when  $\Delta T_{01} < 0.6\text{ K}$ . Owing to subcritical heat addition, the flow is steady. With the increase of  $\Delta T_{01}$ , the condensation zone moves to the front of the throat, and the self-excited oscillation occurs. The oscillation frequency  $f$  decreases monotonically in the cascade, which is quite different to that in general nozzles. The difference is caused by the oscillation mechanism, which is mentioned above, namely the frequency is determined mainly by the supercritical heat addition near the throat at the suction side. As the flow is oscillating, the higher  $\Delta T_{01}$  leads to more upstream condensation process, and the lower Mach number of the subsonic flow, which is heated supercritically, results in a higher required critical heat addition  $Q_c$ . Moreover, due to the expansion rate at the suction side, the condensation intensity decreases with increased  $\Delta T_{01}$ . Therefore, the higher  $\Delta T_{01}$  leads to less supercritical heat addition, and the shock moves upstream more slowly, which results in a lower  $f$ . It can be seen that an increase of  $\Delta T_{01}$  from  $0.6$  to  $9.1$  K results in a decrease of  $f$  from  $93.84$  to  $76.97$  Hz. As  $\Delta T_{01} > 9.1$  K, the flow returns steady due to subcritical heat addition.

#### 4.4. The self-excited oscillation flow at different inlet supercooling

In this section, the self-excited oscillation flow at different inlet supercooling is discussed. For convenience, in oscillating flow the amplitude of mass flow rate and outflow angle refer to the

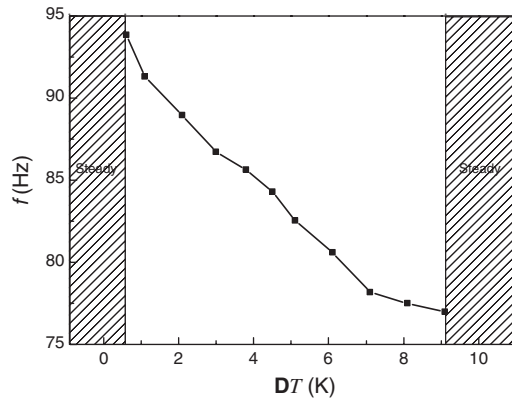


Figure 7. Dependence of oscillation frequency on inlet supercooling for the cascade, with  $p_{01} = 35\ 140\text{ Pa}$ ,  $p_b/p_{01} = 0.38$ .

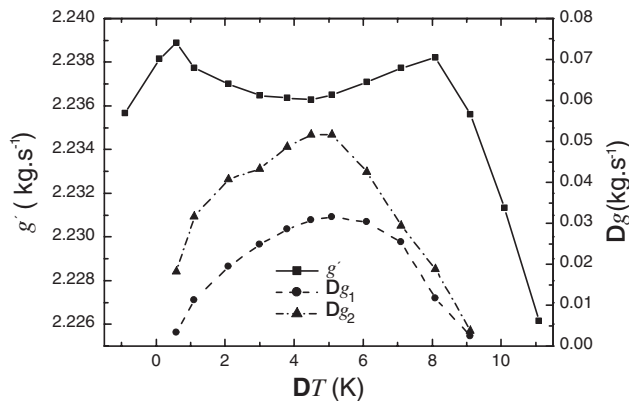


Figure 8. Dependence of the time-averaged value and amplitudes of mass flow rate on inlet supercooling, where  $g'$ ,  $\Delta g_1$  and  $\Delta g_2$  are the time-averaged value, the amplitude at inlet and outlet sections, respectively.

difference between maximum and minimum, while the entropy increase is the difference of time-averaged entropies at the outlet and inlet section.

The time-averaged mass flow rate  $g'$  is given in Figure 8. It can be seen that  $g'$  reaches its peak value as the flow transits from steady to oscillating and  $g'$  in oscillation flow is greater than that in steady flow. It indicates that there is a higher degree of supersaturation in the oscillation flow (it was validated in plenty of experimental work that one of the main effects of supersaturation on wet steam flow is the increase of through-flow), and the periodical compression and expansion of wet steam in the cascade passage suppress the increase of mass flow rate to a certain extent. In addition, the amplitudes of mass flow rate at the inlet and outlet sections ( $\Delta g_1$  and  $\Delta g_2$ ) all increase first and then decrease with increased  $\Delta T_{01}$ . Therefore, the oscillation intensity is enhanced first and weakened afterwards.  $\Delta g_2$  is much greater than  $\Delta g_1$  when  $\Delta T_{01} < 6.1\text{ K}$ , and here the effect of oscillation flow on the outlet section is stronger than that on the inlet one. Otherwise the difference

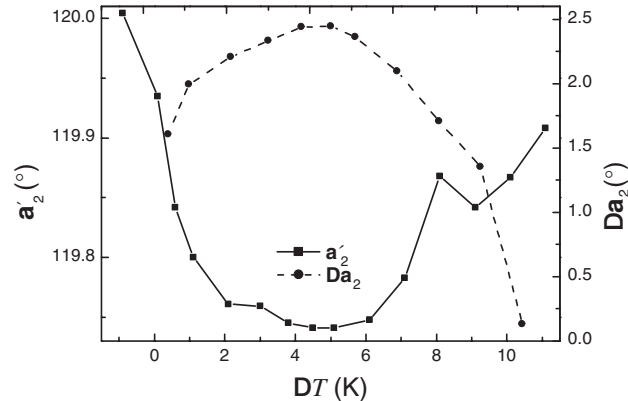


Figure 9. Dependence of time-averaged value and amplitude of outflow angle on inlet supercooling, where  $\alpha_2'$  and  $\Delta\alpha_2$  are the time-averaged value and the amplitude, respectively.

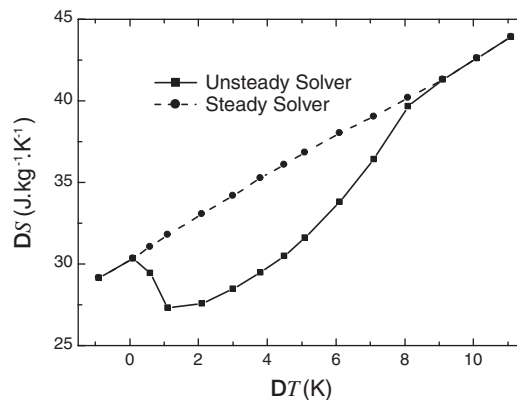


Figure 10. Dependence of entropy increases on inlet supercooling by unsteady and steady solvers, respectively.

between  $\Delta g_1$  and  $\Delta g_2$  is relatively small due to the more upstream condensation zone, and here the effects of oscillation flow on the two previous sections are approximately equivalent.

The self-excited oscillation also leads to periodic change of outflow angle. Figure 9 shows the time-averaged outflow angle  $\alpha_2'$  and the amplitude of outflow angle  $\Delta\alpha_2$ . As shown in Figure 9,  $\alpha_2'$  in the oscillation flow is only slightly less than that in the steady one, but  $\Delta\alpha_2$  is approximately more than  $1.5^\circ$  with its peak value even approaching  $2.5^\circ$ . Therefore, the effect of self-excited flow oscillation on through-flow and stage work should be considered.

The entropy increase  $\Delta S$  versus  $\Delta T_{01}$  is displayed in Figure 10 and steady/unsteady solvers are adopted, respectively. It can be seen that  $\Delta S$  by steady solver is linear with  $\Delta T_{01}$ . The loss in the cascade is mainly caused by condensation indicating that the condensation loss is mainly determined by the position of the condensation zone, in other words the more upstream condensation zone results in more loss. Therefore, the situation that should be avoided in the design of wet

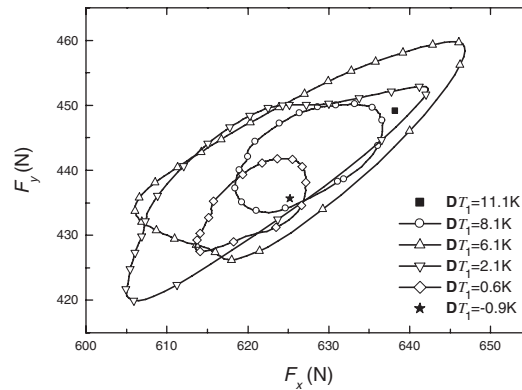


Figure 11. Aerodynamic force on the blade under four oscillating flow conditions and two steady flow conditions, respectively.

steam turbine stages is of a high supercooling at the inlet of cascade where the spontaneous condensation occurs. Moreover,  $\Delta S$  by unsteady solver is less than that by the steady one. It indicates that the condensation loss decreases to a certain extent with the periodical wax and wane of condensation process.

The effect of flow oscillation on blade stress in wet steam flow is worth studying. Supposing that the cascade has unit spanwise height, Figure 11 displays the aerodynamic force on the blade exerted by oscillating flow under four conditions with different inlet supercooling. The axial force  $F_x$  and tangential force  $F_y$  in a cycle are plotted in this figure and compared with those under steady flow conditions. In Figure 11 it can be found that the closed curves of oscillating force on the blade converge at the corresponding point of steady flow, when the oscillating flow transits to steady state with the variation of inlet supercooling.

## 5. THE EFFECTS OF INLET WETNESS AND PERIODIC INLET CONDITIONS

### 5.1. The effects of inlet wetness

With this Eulerian/Eulerian model, the condensation flow with inlet wetness is investigated in this section. Compared with homogeneous condensation, the heterogeneous one occurs under much lower supercooling in the cascade passage. Although the condensation process still departs from equilibrium state to a certain extent, the heat release to transonic flow decreases largely; therefore, the flow is stable. Here, a series of inlet conditions with different wetness or droplet radii is discussed with  $\Delta T_{01} = 1.1$  K.

The parameters of heterogeneous condensation flow with inlet wetness (cases 1–4) are listed in Table II and compared with that of the homogeneous one (case 5). The mass flow rate  $g$ , the axial force  $F_x$ , the tangential force  $F_y$  and the entropy increase  $\Delta S$  are all the time-averaged value of oscillating flow in case 5. It can be seen that the heterogeneous condensation with inlet wetness leads to a decrease of  $g$ , and the flow where  $g$  decreases more is more close to equilibrium state with greater  $Y_1$  or smaller  $r_1$ . Whereas  $F_x$  and  $F_y$  increase in the heterogeneous condensation flow indicating that the flow leans to the pressure side in the cascade passage. In addition, the loss in the

Table II. Parameters of condensation flow with inlet wetness. In cases 1–4 the condensation process is heterogeneous, which is homogenous in case 5.

	$Y_1$	$r_1$ ( $\mu\text{m}$ )	$g$ ( $\text{kg s}^{-1}$ )	$F_x$ (N)	$F_y$ (N)	$\Delta S$ ( $\text{J kg K}^{-1}$ )
Case 1	0.001	0.2	2.225	647.274	448.869	37.149
Case 2	0.001	2.0	2.237	634.765	441.017	37.163
Case 3	0.01	0.2	2.201	689.554	482.372	36.329
Case 4	0.01	2.0	2.235	650.308	449.183	38.598
Case 5	0.0	—	2.238	619.744	438.787	27.309

heterogeneous condensation flow increases by 33.03–41.34%. Therefore, the loss that is caused by the more upstream condensation zone is much greater than the non-equilibrium thermodynamic loss.

### 5.2. The effects of periodic inlet conditions

Owing to the effect of wakes behind stator blades, the temperature at the inlet section of rotor is periodically changing; therefore, the inlet supercooling in rotor cascade varies accordingly relative to the angular speed of the rotor, which is followed by the fact that the oscillating characteristics in the rotor cascade may change essentially. In this section, the effects of periodic inlet conditions are discussed.

For a rotor with an angular speed of 3000 rpm, the frequency of inlet supercooling is  $f_w = 50n$  Hz ( $n$  is the stator blade number) for the rotor cascade. Supposing that the wakes (where the stagnation temperature is  $T_w$  at inlet section) have the same velocity vector as the inlet main flow ( $\Delta T_{01}$ ) of the rotor, and then the range of the wakes acting on the inlet boundary  $\Delta y = \Delta h / \cos \alpha_1$ , where  $\Delta h$  is the wake thickness,  $\alpha_1$  the inflow angle. Therefore, the tangential velocity of wakes relative to the inlet boundary  $v_w = t f_w$ , where  $t$  is the stator pitch. The simulating geometry of the stage is given in Figure 12.

The parameters of oscillation flow with periodic inlet supercooling (cases 1–7) are listed in Table III and compared with that of the steady one (case 8). It can be seen that acting on the rapid condensation zone directly, the upstream wakes with high frequency and low temperature leading to an obvious increase of the oscillation frequency  $f$ . However,  $f$  has a low sensitivity to  $f_w$  when the flow oscillation is mainly caused by supercritical heat addition. In cases 1 and 3,  $f_w$  increases by 50%, while  $f$  only increases by 1.32%. In addition,  $f$  decreases synchronously with  $f_w$  when  $f_w < 500$  Hz, which was found in calculations and is not discussed here.  $\Delta g_1$  decreases to a certain extent due to the periodic inlet supercooling, while its effect on  $\Delta g_2$  is very weak due to the filtration of self-excited oscillation near the throat. Furthermore, the upstream wakes also lead to additional flow losses.

Owing to the direct action, the formation condition of weak self-excited oscillation may be broken; therefore, the limit of steady flow expands. Owing to the weakening of the effect of the upstream wakes on the rapid condensation zone, which is more downstream,  $f$  decreases in spite of lower  $\Delta T_{01}$  and  $\Delta T_w$  in case 4. The self-excited oscillation is so weak that its disturbance in the downstream flow is approximately equivalent to that of the upstream wakes. In Figure 13 the time history of the Mach numbers on points A, B and C is shown for case 4. It can be seen that the self-excited oscillation (501.52 Hz) and the disturbance of the upstream wakes (2500 Hz) are

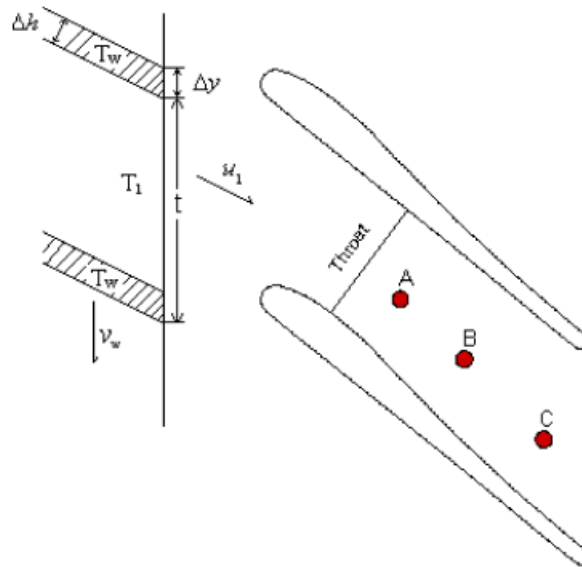


Figure 12. Simplified geometry of the interference between stator and rotor. The tangential velocity of wakes behind stator relative to the inlet boundary of rotor  $v_w = t \cdot f_w$ .

Table III. Parameters of oscillation flow with periodic inlet supercooling.

	$\Delta T_{01}$ (K)	$\Delta T_w$ (K)	$f_w$ (Hz)	$\Delta y$ (mm)	$f$ (Hz)	$\Delta g_1$ ( $\text{kg s}^{-1}$ )	$\Delta g_2$ ( $\text{kg s}^{-1}$ )	$\Delta S$ ( $\text{J kg}^{-1} \text{K}^{-1}$ )
Case 1	4.1	14.1	2500	3.0	537.88	0.0119	0.0532	36.163
Case 2	4.1	14.1	2000	3.0	535.22	0.0113	0.0481	36.16
Case 3	4.1	14.1	3000	3.0	542.28	0.0121	0.0513	36.341
Case 4	1.1	11.1	2500	3.0	501.52	0.0024	0.0087	32.691
Case 5	7.1	17.1	2500	3.0	2481.76	0.0024	0.0054	39.971
Case 6	4.1	19.1	2500	3.0	551.52	0.0121	0.0488	37.137
Case 7	4.1	14.1	2500	4.0	549.86	0.0119	0.0506	36.812
Case 8	4.1	—	—	—	84.96	0.0296	0.0501	29.907

In cases 1–7 the inlet conditions vary with different supercooling in main flow or wakes, frequency of supercooling or thickness of wake; the supercooling at inlet section is uniform and steady in case 8.

coupling. However, the flow parameters in case 5 are fluctuating with a frequency that approaches  $f_w$ , where the self-excited oscillation can be neglected.

The disturbance intensity of the wakes is enhanced with increased  $\Delta T_w$  or  $\Delta y$ ; therefore, the oscillation frequencies all increase in cases 6 and 7.

## 6. CONCLUSION

An Eulerian/Eulerian model has been applied to investigate the unsteady wet steam flow with non-equilibrium condensation. Based on this model, the self-excited oscillation flow in a supersonic turbine cascade is investigated at different inlet supercooling.

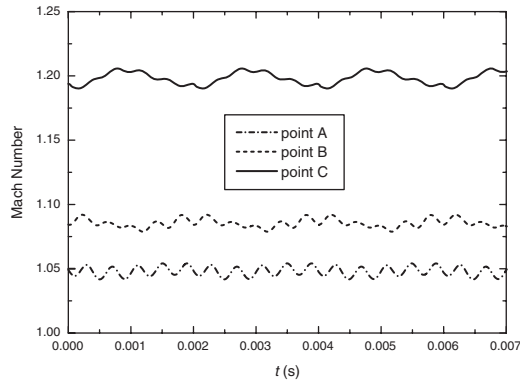


Figure 13. Time history of the Mach number on points A, B and C for case 4, with  $\Delta T_0 = 1.1$  K,  $\Delta T_w = 11.1$  K,  $f_w = 2500$  Hz,  $\Delta y = 3.0$  mm.

Supercritical heat addition in subsonic flow can also lead to self-excited oscillation and secondary condensation may occur downstream. Owing to the special oscillation mechanism and the strong two-dimensional effects on the blade, the oscillation frequency is monotonically decreasing as the inlet supercooling increases. The mass flow rate is greater in the oscillation flow due to the stronger supersaturation, but the periodical compression and expansion of wet steam in the cascade passage suppress the increase. The fluctuation of outflow angle is remarkable. The more upstream condensation zone in the cascade passage results in more loss and the condensation loss in the oscillation flow decreases with the periodical wax and wane of the condensation process.

The heterogeneous condensation with inlet wetness leads to a decrease of the mass flow rate and an increase of the aerodynamic force on the blade. Moreover, the loss that is caused by the more upstream condensation zone is much greater than the non-equilibrium thermodynamic loss.

The high-frequency upstream wakes lead to an obvious increase of the oscillation frequency and additional flow losses. Owing to complexity, the effects of wakes behind stator blades on the self-excited oscillation flow in the rotor cascade need to be investigated further.

#### NOMENCLATURE

$B$	second virial coefficient
$C$	third virial coefficient
$dr/dt$	droplet growth rate
$E$	total specific internal energy of the vapor
$F_N$	aerodynamic force
$F_x$	axial aerodynamic force
$F_y$	tangential aerodynamic force
$f$	frequency
$g$	mass flow rate
$h_t$	total specific enthalpy of the vapor
$h_{fg}$	latent heat
$J$	nucleation rate per unit mass of mixture
$Ma$	Mach number

$\dot{m}$	condensate mass rate per unit mass of mixture
$N$	number of droplets per unit mass of mixture
$p$	pressure
$p_b$	downstream pressure of cascade
$q_j$	heat flux in the $j$ th coordinate direction
$r$	mean droplet radius
$r_c$	Kelvin–Helmholtz critical radius
$t$	time
$T$	temperature, period of oscillation
$T_s$	saturation temperature of the vapor
$u_i, u_j$	velocity components
$x_i, x_j$	spatial coordinates
$Y$	wetness fraction
$\Delta S$	entropy increase
$\Delta T$	vapor supercooling, $(T_s - T)$
$\alpha$	outflow angle
$\rho$	density of mixture
$\rho_g$	density of vapor
$\rho_l$	density of water
$\tau_{ij}$	shear stress
$\phi'$	time-averaged value of scalar $\phi$
$\Delta\phi$	amplitude of scalar $\phi$

*Subscripts*

$i, j$	coordinate direction indices
01	inlet stagnation state
1	inlet
2	outlet
w	upstream wake for rotor

NOTE ADDED IN PROOF

*This article was corrected after initial online publication in the following ways:* The symbol ‘D’ was changed to ‘ $\Delta$ ’ in Tables I, II and III; in Figures 4, 5, 8, 9 and 13; and within the text on pages 6, 8, 10, 11, 12, 13, 14, 15 and 16. The symbol ‘T’ was updated to ‘ $\Delta T$ ’ in Figures 7, 8, 9, 10 and 11. The symbol ‘g’ was changed to ‘ $\Delta g$ ’ in Figure 8. In Figure 9, ‘a’ was changed to ‘ $\alpha$ ’. In Figure 10, ‘S’ was changed to ‘ $\Delta S$ ’.

REFERENCES

1. Barschdorff D, Filippov GA. Analysis of special conditions of the work of laval nozzles with local heat supply. *Heat Transfer—Soviet Research* 1970; **2**(1):76–87.
2. Guha A, Young JB. Time-marching prediction of unsteady condensation phenomena due to supercritical heat addition. *Proceedings Conference Turbomachinery: Latest Development in a Changing Scene*, London, England, 1991; 167–177. ImechE Paper C423/057.



3. Skilling SA, Walters PT, Moore MJ. A study of supercritical heat addition as a potential loss mechanism in condensing steam turbines. *Proceedings of the Institution of Mechanical Engineers International Conference: Turbomachinery—Efficiency Prediction and Improvement*, Cambridge, England, 1987; 125–134. IMechE Paper C259/87.
4. Adam S, Schnerr GH. Instabilities and bifurcation of non-equilibrium two-phase flows. *Journal of Fluid Mechanics* 1997; **348**(1):1–28.
5. Dobkes AL, Zil'ber TM, Kachuriner YY *et al.* Studying the characteristics of wet steam in turbine flow sections. *Thermal Engineering* 1992; **39**(1):45–49.
6. Whirlow DK, McCloskey TJ, Davids J *et al.* Flow instability in low pressure turbine blade passages. *ASME 84-JPGC-GT-14*, 1984.
7. Li L, Sun XL, Li GJ *et al.* Numerical investigation on the self-excited oscillation of wet steam flow in a supersonic turbine cascade. *Progress in Natural Science* 2006; **16**(9):988–992.
8. McCallum M, Hunt R. The flow of wet steam in a one-dimensional nozzle. *International Journal for Numerical Methods in Engineering* 1999; **44**:1807–1821.
9. Moore MJ, Walters PT, Crane RI *et al.* Predicting the fog-drop size in wet-steam turbines. *Institute of Mechanical Engineers Conference Publication*, Warwick, 1973; 101–109.